Dilution monitoring using inline optical emission spectroscopy during Directed Energy Deposition process of aluminium bronze

Malte Schmidt[a,*], Knut Partes[a], Rohan Rajput[b], Giorgi Phochkhua[b], Henry Köhler[b]

[a]Jade University of Applied Sciences, Friedrich-Paffrath-Straße 101, Wilhelmshaven 26389, Germany
[b] DED Services GmbH, Porschestraße 3-5, Helmstedt 38350, Germany

Abstract

In directed energy deposition processes (DED) a sound metallurgical bond is a key quality parameter, which is ensured by controlling the degree of dilution between filler and substrate-material. However, higher dilution within the substrate negatively affects the desired properties and must be monitored. Optical emission spectroscopy is investigated for this purpose. Single tracks using aluminium bronze as filler-material (CuAl9.5Fe1.2) are cladded with varying laser power, onto two substrate-materials i.e. S355 and H11 (1.2343), resulting in varying dilution values. Emission-lines induced by the evaporation of substrate-material (Fe-Cr-Mn) and the filler-material-composition (Cu-Al-Fe) are detected and measured (line-intensity). Line-intensity-ratios, comparing the line-intensities of substrate and filler-material-elements, are correlated with the metallographic results (dilution and chemical composition). An increased degree of dilution leads to a surge in the mixing levels of the substrate and the filler-material within the deposition-tracks. Accordingly, line-intensities of elements inside the substrate increase relative to the filler-material-elements, as represented by the line-intensity-ratios.

Keywords: DED; aluminium bronze; Laser-based Additive Manufacturing; Laser Metal Deposition

1. Introduction and motivation

In directed energy deposition processes (DED) layers of material are added onto a substrate surface or previously deposited layers. This process is used for coating of surfaces as well as repairing and additive manufacturing of industrial components whereby different, specialized materials can be used and combined (DebRoy et al., 2018). Key quality features for the deposition process are a sufficient metallurgical bonding as well as low dilution with the underlying material. However, by increasing the dilution, more material from the underlying layer is mixed into the deposition track. Therefore, the chemical composition is changed, and the desired properties can be negatively affected (Steen and Mazumder, 2010). This was shown for comparing the tribological dry sliding behaviour of aluminium bronze. The powder was deposited on a similar aluminium

bronze alloy and on a steel substrate. Due to the dilution, material from the substrate was mixed into the deposition tracks, resulting in increased friction coefficients for samples using steel substrates (Freiße et al., 2016). As a sufficient bonding and low dilution are particularly important quality features, the ability of monitoring needs to be investigated. Insufficient metallurgical bonding has been investigated by the analysis of optical process emissions using optical emission spectroscopy (OES). Defects (e.g. lack of fusion) during additive manufacturing using DED processes could be detected by the combination of OES and plasma plume imaging. (Stutzman et al., 2018)(Montazeri et al., 2019). The appearance of atomic emission lines within the process emissions is based on the vaporization of alloying elements from the melt pool surface. These element specific emission lines can be detected using OES and assigned to known atomic electron transitions. The vaporization of material depends on the transport of elements to the melt pool surface. Once reaching the surface the temperature and element distribution, the melt pool movement as well as boundary and diffusivity conditions influence the vaporization rate for each element (Collur et al., 1987).

Several studies investigated these process emissions for monitoring of the chemical composition during DED processes. The methodology of those studies follows a comparable pattern. Element specific emission lines are detected and measured in the optical emissions of the process. The intensities of those emission lines are compared by calculating ratios. A series of studies correlated these ratios with the known chemical composition of premixed powder material used in the experiments. Fe-based H13 (1.2344) tool steel mixed with various amounts of pure chromium powder was deposited onto a Fe-based substrate (Song and Mazumder, 2012). By comparing the intensity ratios of neutral Cr- and Fe lines the Cr-content was predicted. The same methodology (Shin and Mazumder, 2018) was used for the prediction of nickel-content during the deposition of powder materials with varying Ni content onto Ni-based material. Another study (Song et al., 2017) investigated multiple calibration methods for the prediction of Al content during the deposition of Al-Ti-powder (mixed out of pure Al and Ti powders) onto Ti-based substrate material. Since these calibrations were based on the composition of the injected powder material, the dilution and mixing with underlying substrate material was not considered. In contrast Wang and Liu (Wang and Liu, 2019) used the chemical composition of the deposition track for the calibration. In the experiments four different Ni-based powders were deposited on a Fe-based substrate and the prediction of the chemical composition has been performed. From the aforementioned literature, it can be derived that the detection and comparison of element emission lines could also be used to monitor dilution and mixing during deposition processes with OES. Therefore, the dilution was intentionally increased by applying higher amounts of laser power during the process. Line intensities of elements exclusively present in the substrate and the powder material were compared. It is hypothesized that the intensity of a substrate element line, representative for its element share, rises relative to a powder element line with increasing degree of dilution.

2. Material and Methods

2.1. Experimental Setup

Single deposition tracks out of aluminium bronze (CuAl9.5Fe1.2) are cladded on sheet metals of H11 (1.2343) hot work tool steel as well as on S355 (1.0570) low alloyed steel using DED. Laser irradiation is delivered from a high-power diode laser (Laserline LDM 4000 60, Laserline GmbH) via an optical fiber (core diameter: 600 µm) to a robot guided processing head. Using a 72 mm collimating lens and a 250 mm focusing lens a circular laser spot with a 2.1 mm diameter is formed. For powder distribution a powder feeder (GTV PF2/2, GTV Verschleißschutz GmbH) is connected to a four-jet powder nozzle (Fraunhofer Coax12V7, Fraunhofer IWS) with a circular powder spot diameter of 2 mm to 3 mm. Argon 4.6 is used as a carrier gas

(3 l/min) as well as shielding gas (15 l/min). The powder feed rate and scan velocity are set to 8 g/min and 1 m/min, respectively. The laser power is varied from 600 W to 2200 W in steps of 200 W (600 W up to 1000 W and 1600 W up to 2200 W) and 100 W (1000 W up to 1600 W). Every experiment is repeated three times.

Optical process emissions are captured with a silicon collimating lens from the area above the melt pool. The lens is connected to a spectrometer (OCEAN HDX-UV-VIS, Ocean Insight) using an optical fiber (diameter: 115 μm). The spectrometer has a resolution of 0.73 nm at FWHM and a bandwidth from 200 nm to 800 nm. Single spectra are recorded back-to-back with a frequency of 100 Hz, resulting in an integration time of 10 ms. A pipe with a blackened inner surface is attached to the collimating lens of the measurement system. A slight flow (4 l/min) of Argon 4.6 is applied to the pipe, in order to prevent contamination of the optical components. It was arranged in a way to not negatively influence the powder flow.

2.2. Materials

The chemical composition of both substrate materials (H11 and S355) is determined by a stationary metal analyzer via arc spark optical emission spectrometry. Measurements are repeated three times and the averaged results are shown in Table 1. The chemical composition of the aluminium bronze powder material is given by the inspection certificate provided by the manufacturer and is also shown in Table 1.

Table 1. Chemical composition of substrate materials H11 and S355 and aluminium bronze powder material METCO 51NS (CuAl9.5Fe1.2)

WT %	C	Fe	Si	Mn	Cr	Mo	V	Cu	Al	Trace particle
H11 (1.2343)	0.41	91.43	1.06	0.4	4.9	1.18	0.36	-	-	Balance
S355 (1.0570)	0.17	98.01	0.23	1.47	-	-	-	-	-	Balance
METCO 51NS (CuAl9.5Fe1.2)	-	1.10	-	-	-	-	-	89.15	9.65	Balance

2.3. Metallographic and chemical composition analysis

For every experiment with varying laser power three separate tracks were deposited on both substrate materials. Cross sections of each track were metallographically prepared to determine the dilution with the underlying substrate material and the chemical composition within the track itself. Tracks are cut orthogonally to the deposition direction, embedded in conductive embedding material (Demotec 70), ground with SiC-paper and polished with a 3 μm diamond suspension. The dilution D defines the ratio of the molten area A1 below the substrate surface and the total of all molten areas (below A1 and above substrate surface A2) of the deposited track. This ratio is described by equation 1 and exemplary cross sections are shown in Fig. 1.

$$D = \frac{A_1}{A_1 + A_2} \qquad\qquad (1)$$

Caused by the dilution of deposited powder and the underlying substrate material the resulting chemical composition of the track also changes. This is measured by energy-dispersive X-ray spectroscopy (EDX) within a scanning electron microscope (SEM). Therefore, a single track is analyzed for each laser power and substrate

material. The chemical composition was averaged within an area in the melted material above the substrate surface on the edge of the track surface. The acceleration voltage was set to 15 kV.

2.4. Spectrometric analysis

During the deposition process single spectra are sequentially recorded and stored. Within these single spectra, intense signals can be detected and assigned to atomic element emission lines. Since several emission lines can be closely neighboured, they cannot be resolved individually. Those signals are therefore referred to as peaks. Those assignments are carried out by the aid of the NIST atomic spectra database (Kramida and Ralchenko, 1999), providing a multitude of known element emission lines throughout the electromagnetic spectrum. Two exemplary spectra are shown in Fig. 3 from deposition processes using H11 and S355 substrate material with a laser power of 2200 W. With the detection of certain peaks, which are assigned to several specific element emission lines, the presence of these elements in the melt pool can be proven as well as the quantity of these elements can be assumed by the intensity of the peak itself. As the dilution influences the chemical composition of the deposition track, the vaporized and excited elements of substrate and powder deposition material can be measured in the spectrometric signals. Detected peaks from elements exclusively present in the substrate (A peaks) and in the powder deposition material (B peaks) can be compared. Therefore, the intensity of peak A (substrate) is divided by the intensity of peak B (powder) and are therefore compared in a peak intensity ratio. This ratio of peak A and peak B respective element A and element B is calculated for each spectrum i within each experiment by equation 2. This ratio can only be calculated if peak A and peak B have been detected in the current spectrum. The average ratio within an experiment can be calculated by the mean intensity ratio. For this, the sum of all ratios is divided by the number n of all ratios. See equation 3.

$$R_{i,A/B} = \frac{I_{i,A}}{I_{i,B}} = \frac{I_{i,Substrate}}{I_{i,Powder}} \tag{2}$$

$$R_{mean,A/B} = \frac{\sum_{i=1}^{n} R_{i,A/B}}{n} = \frac{\sum_{i=1}^{n} \frac{I_{i,A}}{I_{i,B}}}{n} \tag{3}$$

Hence, the total emitted intensity was found to be quite dynamic, the peak intensity was defined as the total intensity of the peak minus the intensity of the background radiation at the measured wavelength. A graphical definition is included in Fig. 3. It is hypothesized that with increasing dilution the peak intensity ratio of substrate- and powder-elements also increases, as more material from the substrate is mixed in the deposition track and can therefore be vaporized.

3. Results and Discussion

3.1. Deposition track dimensions and chemical composition

Each deposition track was metallurgically prepared and the deposited areas above as well as the remelted areas underneath the substrate surface have been measured. The dilution was calculated according to equation 1. This results in three separate dilution values for each substrate material and laser power combination. Fig. 1 shows the averaged dilution of these three values as well as the maximum and minimum values as error bars for each datapoint. The dilution increases continuously with increasing laser power for both substrate materials. The experiments using H11 generally show higher dilution compared to experiments using S355. Cross sections of tracks deposited with 600 W, 1400 W and 2200 W are also shown in Fig. 1. For low laser powers at 600 W and 800 W no dilution could be calculated, as no area underneath the substrate surface was remelted. These tracks have also shown irregular surfaces, not fully melted powder particles as well as partly insufficient bonding to the substrate material.
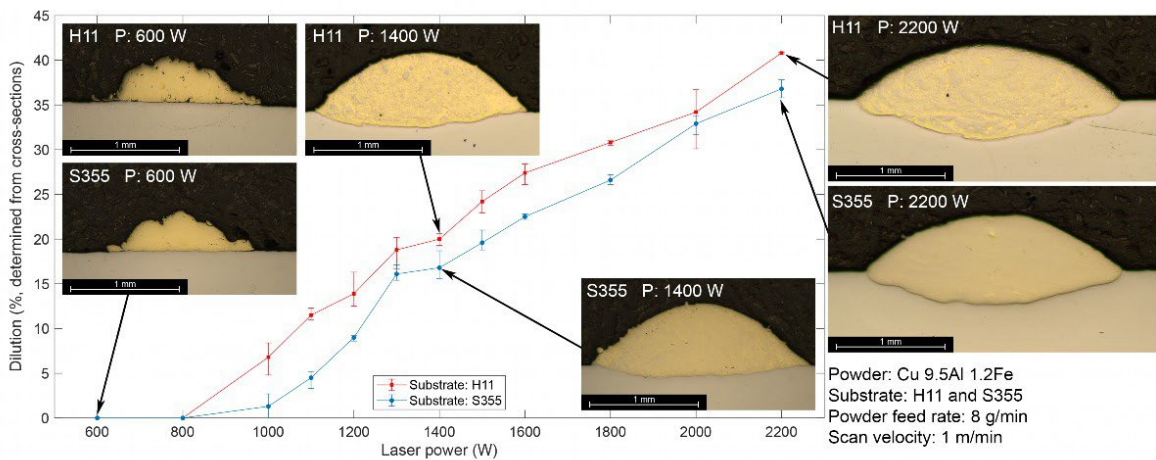

Fig. 1. Mean dilution values for substrate material H11 and S355 with error bars representing maximum and minimum measured values determined from metallographic cross-sections. Exemplary cross section for laser powers at 600 W, 1400 W and 2200 W and constant powder feed rate of 8 g/min and 1 m/min scan velocity.

The chemical composition on the upper area of the deposition track was measured using EDX-analysis. Fig. 2 shows the percentage element share plotted against the varying laser power for H11 (a) and S355 (b) as substrate materials. The measured element share was corrected by excluding carbon due to known sample and SEM contamination effects (Postek, 1996), resulting in unlikely carbon shares of 4-5 wt%. For both diagrams it can clearly be seen that the content of copper and aluminium descends while the content of iron expands with increasing laser power. Substrate specific major alloying elements like chromium (H11) and manganese (S355) show a comparable rising trend. The rising dilution correlates with the increasing or decreasing content of substrate and powder material elements within the deposition track. With higher laser powers more substrate material is melted resulting in higher dilutions. Due to melt pool dynamics this material is mixed into the deposition tracks also reaching the melt pool surface.
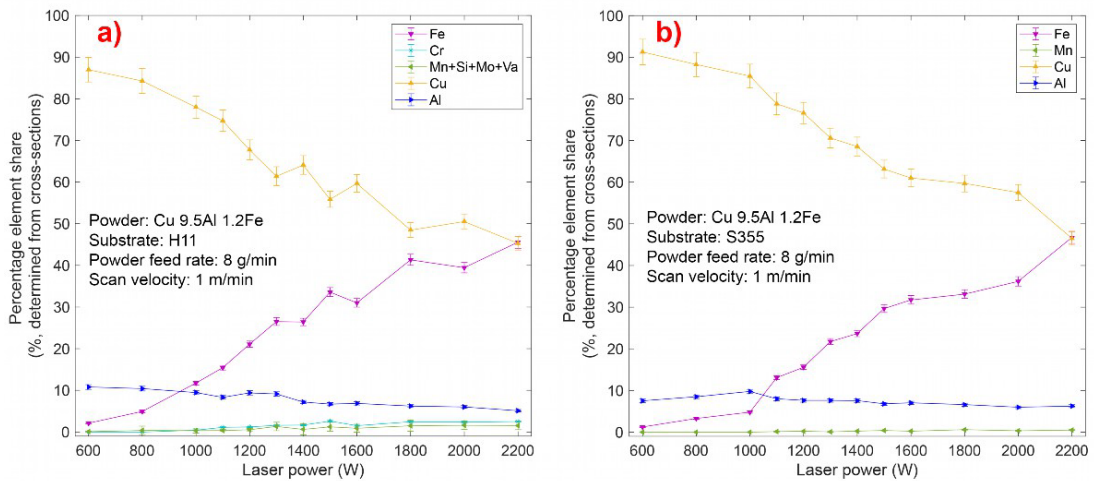
Fig. 2. Percentage element share of the deposition track for (a) substrate material H11 and (b) substrate material S355 determined from metallographic cross-sections.

3.2. Spectrometric peak identification and ratio analysis

Multiple peaks could be detected in the recorded emission spectra and assigned to element emissions lines. Fig. 3 shows two exemplary spectra from deposition processes for both substrate materials using laser power of 2200 W. Several peaks can be detected in both spectra, for example copper at 324.51 nm, 327.25 nm and 510.59 nm assigned to single non-ionized copper emission lines (Cu I) at 324.754 nm, 327.3957 nm and 510.5541 nm (Shenstone, 1948).
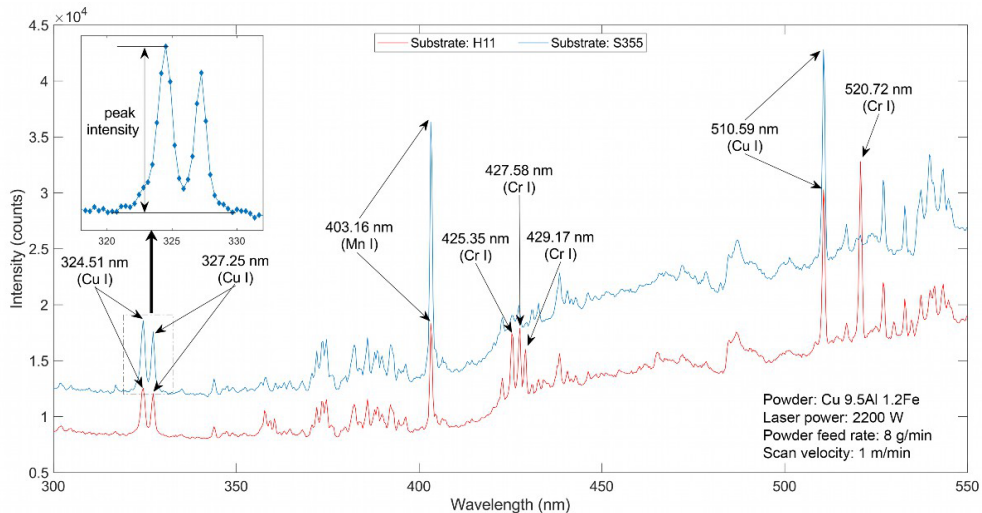

Fig. 3. Exemplary emission spectra for substrate materials H11 and S355 at laser power of 2200 W, powder feed rate of 8 g/min and a scan velocity of 1 m/min

A major manganese peak at 403.16 nm consists of four single Mn I emission lines: 402.644 nm, 403.076 nm, 403.307 nm and 403.449 nm (Meggers et al., 1975). For H11 several chromium peaks can be detected, which are not visible within the S355 spectra. At 425.35 nm, 427.58 nm, 429.17 nm a chromium resonance triplet of non-ionized chromium (Cr I: 425.43517 nm, 427.48117 nm and 428.97307 nm) can be seen. A major peak at 520.72 nm also consists of three narrow neighboured Cr I emission lines (520.44981 nm, 520.60229 nm, 520.84094 nm) (Wallace and Hinkle, 2009). Due to the narrow distance the spectrometer cannot resolve the separate lines. Previous DED experiments (Schmidt et al., 2023) with Cr-Mn-containing material have verified the presence of these Cr I lines at 520.72 nm as well as Mn I lines at 403.16 nm.

For the calculation of peak intensity ratios, the intensity of the Cu I peak at 324.51 nm is used as indicator for the powder material (peak B) for both substrate materials. For substrate material H11 the Cr I peak at 520.72 nm and for S355 the Mn I peak at 403.16 nm is used (peak A). Ratios are calculated for every single spectrum in each experiment. All ratios of the three experiments for each laser power are combined and illustrated in a box plot in Fig. 4. The box plot represents the statistical distribution of the calculated values. The median value of all ratios is represented as horizontal line. The box above and underneath the median line includes 50% (±25%) of the ratio values – interquartile range. The whiskers show the highest and lowest value, respectively, excluding the outliers, defined as values with a range of more than 1.5-times the interquartile range from the top or bottom edge of the box. These individual datapoints are represented with crosses.
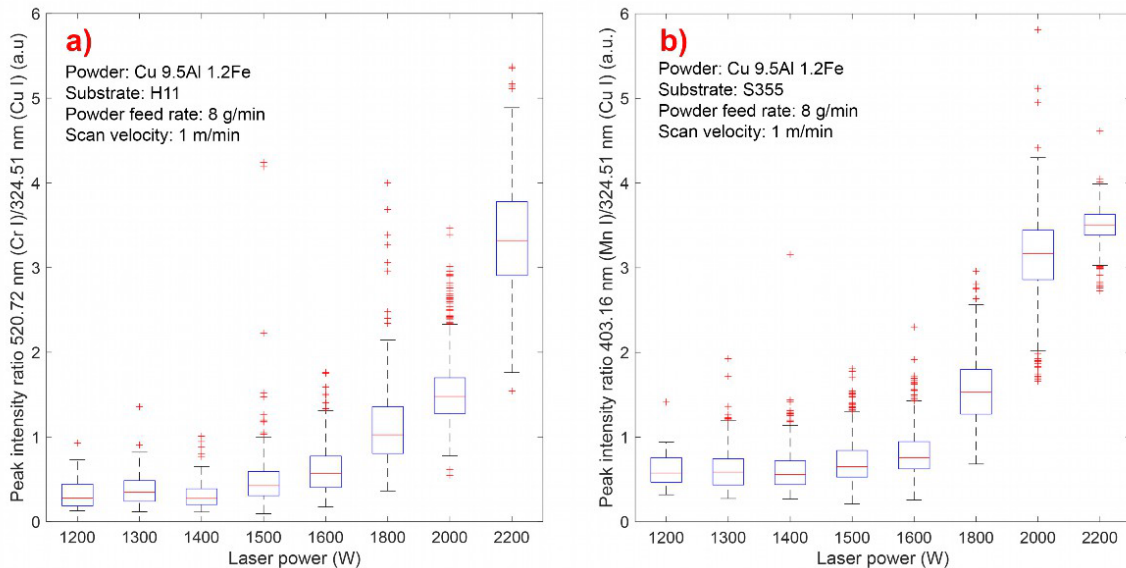

Fig. 4. Box plots of peak intensity ratio for (a) substrate material H11 using peaks 520.72 nm (Cr I)/324.51 nm (Cu I) and (b) substrate material S355 using peaks 403.16 nm (Mn I)/324.51 nm (Cu I)

Peaks could only be found for laser powers of 1200 W and rising. Below this threshold only minor element emissions occur and therefore no ratios can be calculated. This can be observed for both substrate materials. In the region between 1200 W and 1400 W the median value deviates on a comparable level. The values and number of outliers increases slightly. With further increase of the laser power the median values increase rapidly as well as the boundaries of boxes and whiskers also increase.

3.3. Dilution and mixing correlations to spectral signals

Comparing the trends of dilution values, chemical composition and element specific spectrometric signals during laser power variations, a correlation can be observed in Fig. 1, Fig. 2 and Fig. 4. Elements exclusively present in the substrate material (Cr for H11 and Mn for S355) have been detected within the deposition track by both the spectral emissions as well as the EDX-analysis. This verifies the effect of mixing during the deposition process caused by the dilution of substrate and powder material. As the share of substrate material elements, mainly iron as well as additional alloying elements (Cr and Mn), increase due to increasing dilution, the ratios of peak intensities of these corresponding elements (Cr I/Cu I and Mn I/Cu I) also increase. Fig. 5 shows the resulting dilution plotted against the mean peak intensity ratio for each single experiment using H11 (a) and S355 (b) achieved by different levels of laser power at otherwise constant process parameters. A correlation of these resulting values can also be observed. For both substrate materials the average peak intensity ratio can only be detected for dilution values slightly below (S355) or above (H11) 10%. From that point on the peak ratio increases with the degree of dilution. As the dilution corresponds directly to the applied laser power the effects of vaporization and excitation for each element have to be taken into account.
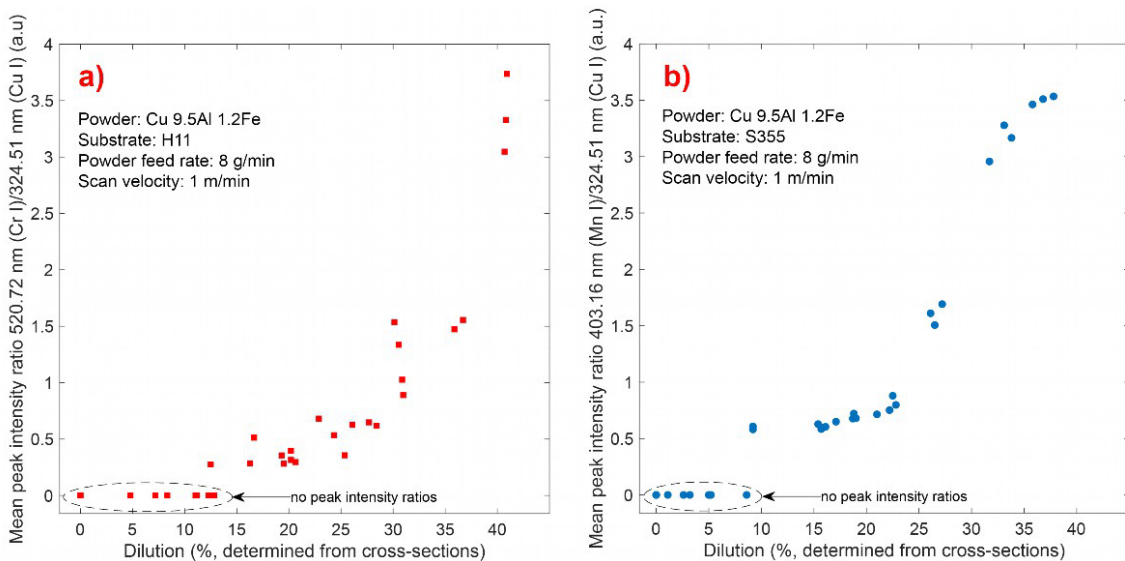

Fig. 5. Mean peak intensity ratios for (a) substrate material H11 using peaks 520.72 nm (Cr I)/324.51 nm (Cu I) and (b) substrate material S355 using peaks 403.16 nm (Mn I)/324.51 nm (Cu I) plotted against the dilution of the deposited track determined from metallographic cross-sections.

4. Conclusion

DED experiments depositing aluminium bronze powder onto two different Fe-based substrate materials with varying laser powers have been conducted. Process emissions have been captured with a spectrometer and element specific element emission lines have been detected and identified. The dilution values of all deposition tracks have been measured and calculated as well as the chemical compositions were measured within metallographic cross sections using EDX. The following findings could be concluded:

- Increasing laser power with constant powder feed rate and scan velocity increases the dilution of single deposition tracks. At identical process parameters hot work tool steel H11 shows slightly

> higher dilution compared to S355 substrate material, associated to lower melt temperature and lower thermal conductivity.

- With increasing dilution, the share of elements (Fe, Mn, Cr), which are originated from the substrate material, increases within the deposition tracks. Thus, the mixing of both materials can be verified.
- Using OES multiple peaks could be assigned to element emission lines of Cu, Cr and Mn. Peak intensity ratios, representing substrate to powder material relation, showed a correlation to the degree of dilution and the share of elements within the deposition tracks.
- The vaporization and thus the detection of element emission lines is mainly influenced by the applied laser power or intensity of the laser irradiation. Element specific emission lines could only be detected up from 1200 W laser power. Those mechanisms may superimpose the ratio of peak intensities and therefore the monitoring of mixing and dilution effects.

However, OES shows great potential for the monitoring of mixing and dilution during DED processes. As several studies have also investigated additional monitoring and control possibilities, OES could be used as a multi-purpose sensor system. Further investigation on element specific vaporization mechanisms is needed to improve the use of OES as a flexible monitoring system.

References

Collur, M. M.; Paul, A.; DebRoy, T., 1987.: Mechanism of alloying element vaporization during laser welding. Metallurgical Transactions B 18 (4), p. 733.

DebRoy, T.; Wei, H. L.; Zuback, J. S.; Mukherjee, T.; Elmer, J. W.; Milewski, J. O. et al., 2018.: Additive manufacturing of metallic components – Process, structure and properties. Progress in Materials Science 92, p. 112.

Freiße, H.; Langebeck, A.; Köhler, H.; Seefeld, T.; Vollertsen, F., 2016.: Investigations on dry sliding of laser cladded aluminum bronze. Manufacturing Review 3, p. 13.

Kramida, A.; Ralchenko, Y., 1999.: NIST Atomic Spectra Database, NIST Standard Reference Database 78.

Meggers, W. F.; Corliss, C. H.; Scribner, B. F., 1975.: Tables of spectral-line intensities. Nat. Bur. Stand.

Montazeri, M.; Nassar, A. R.; Stutzman, C. B.; Rao, P., 2019.: Heterogeneous sensor-based condition monitoring in directed energy deposition. Additive Manufacturing 30, p. 100916.

Postek, M. T., 1996.: An approach to the reduction of hydrocarbon contamination in the scanning electron microscope. Scanning 18 (4), p. 269.

Schmidt, M.; Gorny, S.; Rüssmeier, N.; Partes, K., 2023.: Investigation of Direct Metal Deposition Processes Using High-Resolution In-line Atomic Emission Spectroscopy. Journal of Thermal Spray Technology 32 (2-3), p. 586.

Shenstone, A. G., 1948.: The first spectrum of copper (Cu I). Phil. Trans. R. Soc. Lond. A 241 (832), p. 297.

Shin, J.; Mazumder, J., 2018.: Composition monitoring using plasma diagnostics during direct metal deposition (DMD) process. Optics & Laser Technology 106, p. 40.

Song, L.; Huang, W.; Han, X.; Mazumder, J., 2017.: Real-Time Composition Monitoring Using Support Vector Regression of Laser-Induced Plasma for Laser Additive Manufacturing. IEEE Transactions on Industrial Electronics 64 (1), p. 633.

Song, L.; Mazumder, J., 2012.: Real Time Cr Measurement Using Optical Emission Spectroscopy During Direct Metal Deposition Process. IEEE Sensors Journal 12 (5), p. 958.

Steen, William M.; Mazumder, Jyotirmoy, 2010.: Laser Material Processing. London: Springer London.

Stutzman, C. B.; Nassar, A. R.; Reutzel, E. W., 2018.: Multi-sensor investigations of optical emissions and their relations to directed energy deposition processes and quality. Additive Manufacturing 21, p. 333.

Wallace, L.; Hinkle, K., 2009.: THE 236.6–5400.0 nm SPECTRUM OF Cr I. ApJ 700 (1), p. 720.

Wang, S.; Liu, C., 2019.: Real-Time Monitoring of Chemical Composition in Nickel-Based Laser Cladding Layer by Emission Spectroscopy Analysis. Materials (Basel, Switzerland) 12 (16).